

[2129] RC はりの衝撃挙動解析と付着特性のモデル化に関する研究

NON-LINEAR ANALYSIS AND BOND MODELLING OF RC BEAMS SUBJECTED TO IMPULSIVE LOADS

Ayaho MIYAMOTO* and Michael William KING*

1. INTRODUCTION

The use of concrete in nuclear reactors, marine structures and other large structures are getting quite common nowadays. When considering such structures which are exposed to very severe conditions, the effects of impacts has to be taken into account. At present, the characteristics of impact forces as well as the behaviour of structures prior to failure have yet to be made clear. In this study, a dynamic non-linear finite element analytical approach was used to study the behaviour of RC beams subjected to impulsive loads up to failure. It was found that a proper bond model is necessary to study the mechanical behaviour of structures in the elasto-plastic region. The main purpose of this study is to modelize bond characteristics between concrete and reinforcement, especially under impulsive loads, in order to obtain a more accurate method of analysis. The linkage element (bond-link element) developed by Ngo and Scordelis(1) was employed in the analysis.

2. DESCRIPTION OF SPECIMENS AND TESTS

A series of static and dynamic (impulsive) tests were carried out to study the effects of reinforcement bar type and loading rates on bond.

2.1 TEST SPECIMENS

The specimens used in these tests had an overall dimension (length x width x depth) of 1,300 x 150 x 150 mm. A metal hinge was placed in the compression side at the centre of the beam specimen to induce tensile action in the bottom reinforcing bar (test bar) during loading. Details of the specimens are shown in Fig.1. Two types of test bars were used (D13 and D16, deformed bar) together with a combination of three types of rubber pad depth (6,10 and 20cm). Uniaxial and biaxial wire strain gauges were placed in the centre of the test bars to measure both the strain along the bars (horizontal direction) and in the direction perpendicular to bar axis (vertical direction). Details of the test bars are shown in Fig.2. Mould gauges were also embedded in concrete directly opposite to the biaxial strain gauges (see Fig.1). The aim of placing these mould gauges is to

*Department of Civil Engineering, Faculty of Engineering, Kobe University

measure concrete strain at the steel-concrete surface.

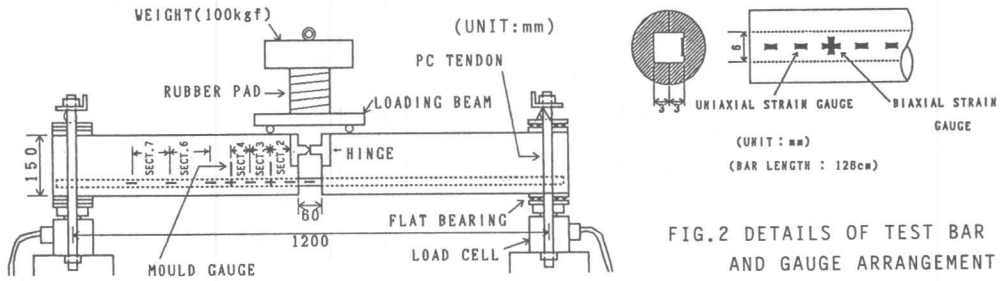


FIG.1 DETAILS OF SPECIMEN AND IMPACT TEST SET-UP

FIG.2 DETAILS OF TEST BAR AND GAUGE ARRANGEMENT

2.2 TEST PROCEDURES

Static tests were carried out using a 200tf universal testing machine with a simple support span of 1,200mm. The loading set-up for impulsive tests is shown in Fig.1. PC tendons were tightened at both of the supports to prevent the ends from lifting off during impulsive loading. A rubber pad was placed above the loading beam at midspan to vary the loading rate. A weight of 100kgf was then dropped from various heights at midspan to induce impulsive force. Altering the rubber depth and the falling height of weight allows various impulsive forces and impulsive load durations to be obtained. It was found that the impulsive load duration varied only with the depth of rubber pad and test bar type (see Table 1). The range of loading rates for impulsive test was between 1.42×10^4 kgf/sec and 10.2×10^4 kgf/sec.

TABLE 1 AVERAGE IMPULSIVE LOAD DURATION (ms)

TEST BAR	DEPTH OF RUBBER PAD (cm)		
	6	10	20
D13	29.0	32.0	36.0
D16	23.0	27.0	34.0

3. TEST RESULTS AND DISCUSSIONS

3.1 STRAIN DISTRIBUTION

Some typical results of strain distribution along the test bar are shown in Figs.3 and 4. Fig.3 shows the strain distribution of a D16 bar under static loading while Fig.4 is that of a D13 test bar with a 6cm rubber pad under impulsive loads. It is clear that the strain distribution for these two types of tests are different. Under static loading, strain is proportionally distributed along the bar length. On the other hand, under impulsive loading, there is a tendency for high strain concentrations to occur near the midspan while values near the supports are quite negligible.

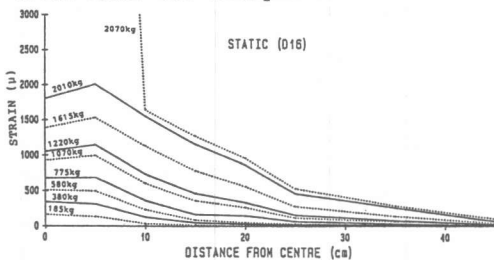


FIG.3 STRAIN DISTRIBUTION (STATIC)

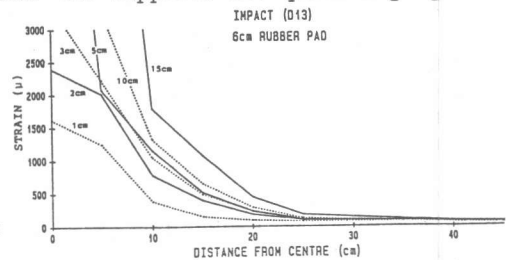


FIG.4 STRAIN DISTRIBUTION (IMPACT)

From the test results, it can be concluded that as the loading rate increases, impulsive loading produces a bond behaviour that is different from that of static loading.

3.2 BOND STRESS-SLIP DISTRIBUTION

Bond stress as well as local slip were calculated from strain distribution along the test bars. In the calculations, slip at the measured point nearest to the support was considered to be zero. Bond stress was based on the assumption that the horizontal forces acting in the test bar direction changed linearly between measured points. Local slip was considered as a function of bond stress and integrating this function provided local slip. Some typical results from these calculations are shown in Figs.5-8. The first two figures show a relation of bond stress-local slip using the conventional method. Here, the conventional method refers to local slip at various sections in the direction of bar axis being plotted against bond stress while under different loads. The sections between alternate strain gauges from midspan is taken as Sects.1-7 respectively (Refer Fig.1). Sect.1 is not shown in the figures because part of the section is exposed from concrete coverage.

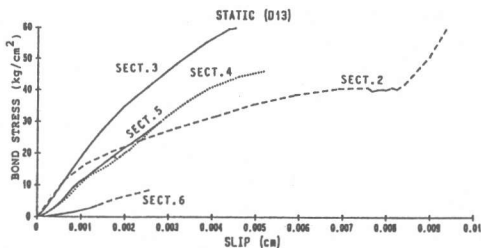


FIG. 5 STATIC RESULT FROM CONVENTIONAL METHOD

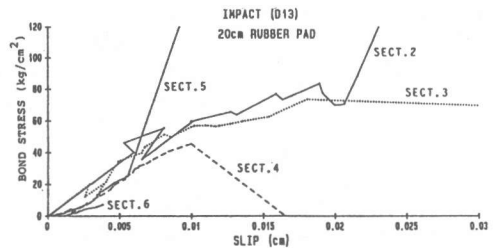


FIG. 6 IMPACT RESULT FROM CONVENTIONAL METHOD

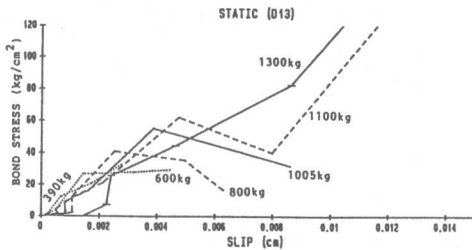


FIG. 7 STATIC RESULT FROM PROPOSED METHOD

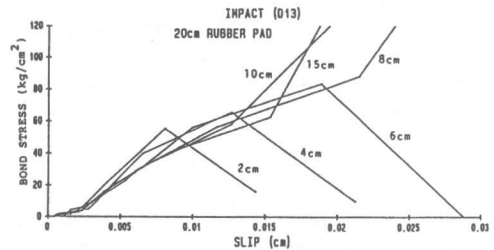


FIG. 8 IMPACT RESULT FROM PROPOSED METHOD

The following two figures also show the bond stress-local slip relationships but was obtained from a different approach. In this approach, bond stress-local slip along test bar for each load was plotted on a different curve. It can be noticed that in the conventional method, the initial gradient varies widely and thus, the amount of error in determining the gradient is large. But using the proposed approach, it is clear that regardless of the difference in loading rates and bar type, there is linearity in the curves below a certain level of bond stress. Besides that, the gradients are roughly the same, allowing a much smaller degree of error to occur. The gradient obtained from this approach is found to be roughly equivalent to the average gradient values from the conventional method (Refer Table 2). It can be concluded that the curve gradient from the proposed approach gives a more accurate result. This is the main merit of this approach.

From Figs.5 and 6, it can be observed that under impulsive loading, the initial curve gradient is smaller than that of static loading but bond failure only occurs at a value larger than that of static loading.

TABLE 2 COMPARISON OF INITIAL CURVE GRADIENT (K_h VALUE)

TEST TYPE	TEST BAR	DEPTH OF RUBBER PAD	CURVE GRADIENT (kgf/cm ²)			
			CONVENTIONAL METHOD			PROPOSED METHOD
			MAX.	MEAN	MIN.	
STATIC	D13	----	19000	10800	3600	12300
STATIC	D16	----	18500	7000	2500	8670
IMPACT	D13	8cm	8600	7300	2000	6500
IMPACT	D13	10cm	6650	6500	1000	7070
IMPACT	D13	20cm	7000	5400	1500	5300
IMPACT	D16	8cm	5300	5000	1100	7800
IMPACT	D16	10cm	5300	3900	1250	3600
IMPACT	D16	20cm	4500	3500	1000	4800

3.3 BOND MODEL

In this study, the linkage element (bond link element) was used to model the bond characteristics between concrete and reinforcement. The mechanism of bond can be attributed to 2 main factors, namely chemical bond and mechanical interlock between concrete and reinforcement. The chemical bond is believed to be destroyed at an early stage. Therefore, the mechanical interlock is the main action operating at the contact surface.

To simulate the effect of bond slip, the bond link element is placed between the concrete and steel nodes in the finite elements. Bond link elements are represented by two springs which have no physical dimensions, one in the bar axis direction (K_h) and the other in the bar radial direction (K_v). The spring stiffness shows the degree of bond stiffness acting between concrete and steel.

Spring stiffness in the direction of bar axis (K_h) is usually derived from the initial gradient of bond stress-local slip relation mentioned in the previous section. Numerical values are shown in Table 2. It was found that the average values from the conventional method can be expressed as a function of variables of this tests, that is the loading rate and the bar type. The function is assumed as,

$$K_h = f(\psi, t) \tag{1}$$

where, ψ is the bar circumference (cm) and t is the average impulsive load duration (sec). Based on the test results, the following equation was obtained.

$$K_h = \log_{10} (\psi \cdot t) \tag{2}$$

This relationship is shown in Fig.9. Fig.10 shows a typical example of an idealized bond stress-local slip for static and impulsive tests.

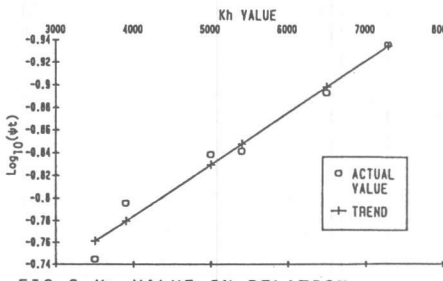


FIG.9 K_h VALUE IN RELATION WITH PARAMETERS

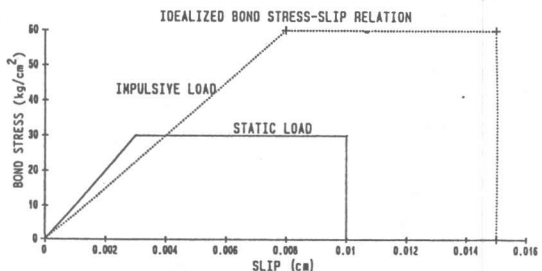


FIG.10 IDEALIZED BOND STRESS-SLIP RELATION

On the other hand, the spring stiffness in the direction perpendicular to bar axis (K_v) is always assumed as a relatively large value compared to K_h . In this study, an attempt was made to obtain the value of K_v through the experiment. The spring stiffness (K_v) was calculated from the difference in stress at the steel-concrete surface. In other words, strain measured at the mould gauge (strain in concrete) and the biaxial strain gauge (strain in steel, bar radial direction) was used to calculate the value of K_v . An example of this result is shown in Fig.11. From the values obtained, it is found that $K_v=1.1 \times 10^6 \text{ kgf/cm}^3$, a value slightly smaller than assumed in previous studies.

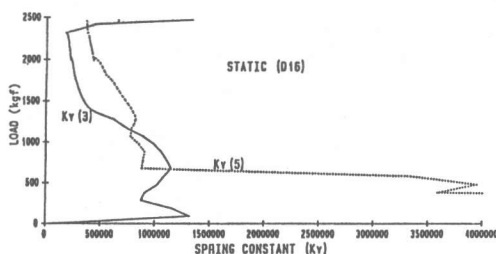


FIG.11 K_v VALUE IN RELATION WITH LOAD

From the values obtained, it is found that $K_v=1.1 \times 10^6 \text{ kgf/cm}^3$, a value slightly smaller than assumed in previous studies.

4. METHOD OF ANALYSIS

The above-mentioned bond model as well as the spring constants derived were included into the non-linear finite element analysis. Loading rates and spring constant values were altered to study the effects on the analysis of a normal RC beam.

Basically, two types of analysis were carried out. The first was under loading in the elastic stage (hysteresis curve) up to 1.2tf while the other was under loading up to failure. Here, failure is defined as the stage where concrete at the compressed region fails (ultimate compressive strain exceeds 3500μ). As for the loading rates, two types of loading rates were considered, a relatively slow loading rate (L) and a relatively fast loading rate (H).

4.1 ANALYSIS IN THE ELASTIC STAGE

The load-deflection relation from this analysis is shown in Fig.12. In the elastic stage, the effect of spring stiffness is quite negligible. Therefore, the effect of loading rates is only considered. From Fig.12, it is clear that as the rate increases, the stiffness of the beam in the initial stages increases too but there is a delay in time between maximum load and maximum deflection.

4.2 ANALYSIS OF FAILURE MODE

To study the effects of spring stiffness on beam behaviour, three values representing different conditions were used. Numerical example of such values is given below:

- 1) Complete bond $K_h : 2.0 \times 10^8 \text{ kgf/cm}^3$
 - 2) Experimental result $K_h : 7300 \text{ kgf/cm}^3$
 - 3) Unbonded $K_h : 20 \text{ kgf/cm}^3$
- The value of K_v was set at $1.1 \times 10^6 \text{ kgf/cm}^3$.

Fig.13 shows the load-deflection relation. Effects of spring stiffness only becomes noticeable once the elasto-plastic stage is reached. When the value of K_h gets smaller, the maximum displacement at failure tends to be larger. But in the case of static loading, the unbonded beam behaves

differently from the others with a practically low degree of stiffness from the beginning. As for the other two beams, a difference in behaviour is only observed after exceeding the elastic stage.

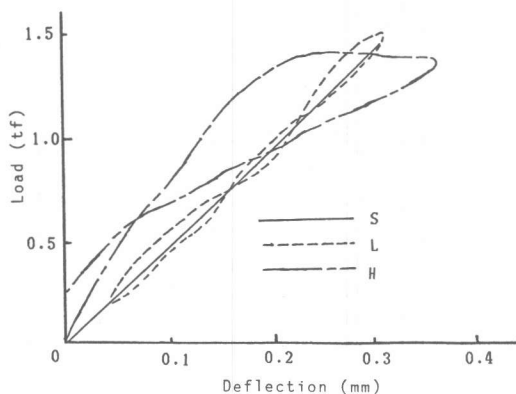


FIG. 12 LOAD-DEFLECTION HYSTERESIS WITHIN ELASTIC STAGE

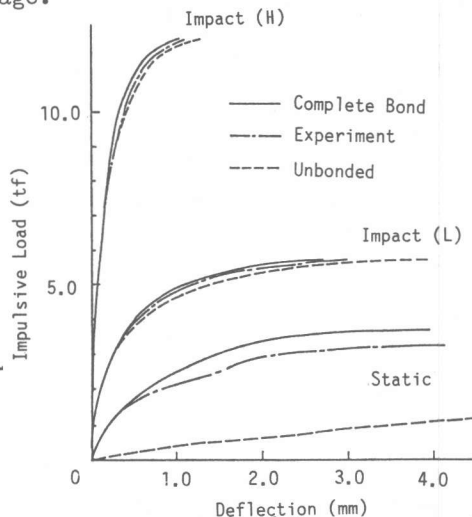


FIG. 13 LOAD-DEFLECTION CURVE UP TO FAILURE

Next, we shall take into account the effect of loading rates on these results. From Fig.13, increase in the loading rate causes inertial effects to be more distinctive. The maximum impulsive force also increases while the maximum displacement has a tendency of being smaller. These results are in close agreement with the test results.

The difference between static and impulsive behaviour can be observed in the elasto-plastic stages where a sudden drop in stiffness occurs only in the case of impulsive loading.

5. CONCLUSIONS

This study was aimed at providing a bond model between concrete and reinforcement for structures under impulsive loading. The bond model was applied into a dynamic non-linear finite element analysis with the intention of application towards a new design concept for structures withstanding impulsive forces. With loading rate and bar type as variables, a series of tests were carried out and then analysis on RC beams were carried out to determine the validity of the model obtained.

The conclusions derived from this study can be summarized as follows:

- (1) Under impulsive loading, the initial curve gradient is smaller than that of static loading but bond failure occurs at a value larger than that of static loading.
- (2) The spring stiffness in the direction of bar axis (K_h) can be expressed as a function of bar circumference and average impulsive load duration.
- (3) When considering impulsive action, the necessity to consider a reasonable bond model arises only after exceeding the elastic range.

REFERENCES

- 1) Ngo, D. and Scordelis, A.C.: "Finite Element Analysis of Reinforced Concrete Beams", ACI Journal, March 1967, pp.152-163